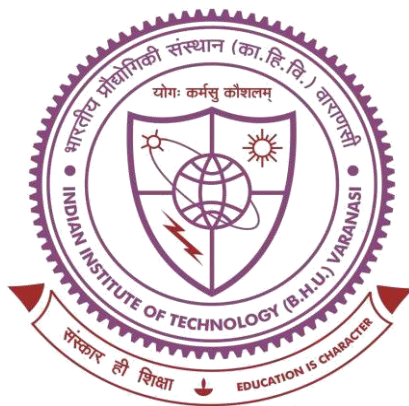


Layer, Morphology and Substrate Dependent Anisotropic,  
Thermal and SERS Studies of CVD Grown 2H-MoS<sub>2</sub>



Thesis submitted in partial fulfilment  
for the Award of

*Doctor of Philosophy*

By

*Ankita Singh*

SCHOOL OF MATERIALS SCIENCE AND TECHNOLOGY  
INDIAN INSTITUTE OF TECHNOLOGY  
(BANARAS HINDU UNIVERSITY)  
VARANASI - 221005  
INDIA

Roll no.: 18111002

Year: 2024



भारतीय  
प्रौद्योगिकी  
संस्थान  
काशी हिन्दू विश्वविद्यालय



INDIAN  
INSTITUTE OF  
TECHNOLOGY  
BANARAS HINDU UNIVERSITY

## CERTIFICATE

It is certified that the work contained in the thesis titled “*Layer, Morphology and Substrate Dependent Anisotropic, Thermal and SERS Studies of CVD Grown 2H-MoS<sub>2</sub>*” by Ankita Singh has been carried out under my supervision and that this work has not been submitted elsewhere for a degree.

It is further certified that the student has fulfilled all the requirements of comprehensive examination, candidacy and SOTA for the award of the Ph.D. degree.

Date: 26-02-2024

Place: Varanasi

**Dr. Ashish Kumar Mishra**  
(Supervisor)

**School of Materials Science & Technology**  
**Indian Institute of Technology**  
**(Banaras Hindu University)**  
**Varanasi**

Associate Professor/सह-आचार्य  
School of Materials Science & Technology/पदार्थ विज्ञान एवं प्रौद्योगिकी स्कूल  
Indian Institute of Technology/भारतीय प्रौद्योगिकी संस्थान  
(Banaras Hindu University), Varanasi/काशी हिन्दू विश्वविद्यालय, वाराणसी



भारतीय  
प्रौद्योगिकी  
संस्थान  
काशी हिन्दू विश्वविद्यालय




INDIAN  
INSTITUTE OF  
TECHNOLOGY  
BANARAS HINDU UNIVERSITY

### DECLARATION BY THE CANDIDATE

I, "**Ankita Singh**", certify that the work embodied in this thesis is my own bonafide work carried out by me under the supervision of "**Dr. Ashish Kumar Mishra**" from "**July 2018**" to "**February 2024**", at the "**School of Materials Science and Technology**", Indian Institute of Technology (BHU), Varanasi, India. The matter embodied in this thesis has not been submitted for the award of any other degree/diploma. I declare that I have faithfully acknowledged and given credits to the research workers wherever their works have been cited in my work in this thesis. I further declare that I have not willfully copied any other's work, paragraphs, text, data, results, *etc.*, reported in journals, books, magazines, reports dissertations, thesis, *etc.*, or available at websites and have not included them in this thesis and have not cited as my own work.


Date...26-02-2024...

Place: Varanasi

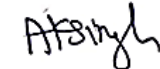
  
(Ankita Singh)

### CERTIFICATE BY THE SUPERVISOR

This is to certify that the above statement made by the candidate is correct to the best of my knowledge-

  
**Dr. Ashish Kumar Mishra**  
(Supervisor)  
School of Materials Science & Technology  
Indian Institute of Technology  
(Banaras Hindu University)  
Varanasi

Associate Professor/सह-आचार्य  
School of Materials Science & Technology/पदार्थ विज्ञान एवं प्रौद्योगिकी स्कूल  
Indian Institute of Technology/भारतीय प्रौद्योगिकी संस्थान  
(Banaras Hindu University), Varanasi/काशी हिन्दू विश्वविद्यालय, वाराणसी

  
(Coordinator)  
School of Materials Science & Technology  
Indian Institute of Technology  
(Banaras Hindu University)  
Varanasi

Coordinator/समन्वयक  
School of Materials Science & Technology/पदार्थ विज्ञान एवं प्रौद्योगिकी स्कूल  
Indian Institute of Technology/भारतीय प्रौद्योगिकी संस्थान  
(Banaras Hindu University), Varanasi/काशी हिन्दू विश्वविद्यालय, वाराणसी



भारतीय  
प्रौद्योगिकी  
संस्थान  
काशी हिन्दू विश्वविद्यालय



INDIAN  
INSTITUTE OF  
TECHNOLOGY  
BANARAS HINDU UNIVERSITY

## COPYRIGHT TRANSFER CERTIFICATE

**Title of the Thesis:** *Layer, Morphology and Substrate Dependent Anisotropic, Thermal and SERS Studies of CVD Grown 2H-MoS<sub>2</sub>*

**Name of the Student:** *Ankita Singh*

### Copyright Transfer

The undersigned hereby assigns to the Indian Institute of Technology (Banaras Hindu University) Varanasi all rights under copyright that may exist in and for the above thesis submitted for the award of the “*DOCTOR OF PHILOSOPHY*”.

Date: 26-02-2024

Place: Varanasi

  
(Ankita Singh)

**Note:** However, the author may reproduce or authorize others to reproduce material extracted verbatim from the thesis or derivative of the thesis for author's personal use provided that the source and the Institute's copyright notice are indicated.

## Acknowledgements

Even though the title page of this thesis only lists one name, several people were involved in its acquisition. First and foremost, I want to thank God Almighty for all the privileges and possibilities He has given me throughout my life. I would like to express my sincere gratitude to my esteemed supervisor **Dr. Ashish Kumar Mishra** for all the fruitful scientific discussions and insightful comments throughout my Ph.D. work. Without his constant monitoring, valuable time, guidance and cooperation, I would not have been able to complete my Ph.D. thesis successfully. His supportive nature has significantly fueled my motivation in work. His patience and excitement during my training are beyond description, and I will forever be grateful to him.

I would also like to express my sincere thanks to my RPEC members Dr. Sanjay Singh, School of Materials Science & Technology, IIT (BHU) and Dr. Sunil Kumar Singh, Department of Physics, IIT (BHU), for their significant scientific discussion and appreciation during the whole journey. I would like to thank present and previous coordinators of School of Materials Science and Technology, IIT (BHU), for providing instrumental facility and cooperation during my Ph.D. I wish to express deep regards to all the teachers of the Department Prof. D. Pandey, Prof. P. Maiti, Prof. R. Prakash, Dr. C. Rath, Dr. A. K. Singh (Coordinator), Dr. C. Upadhyay, Dr. B. N. Pal, Dr. S. K. Mishra, Dr. N. Kumar, Dr. R. Panwar and Dr. A. Kumar for their inspiration and kind support.

With a deep sense of gratitude, I express my sincere thanks to CIFC, IIT (BHU), Varanasi for help in carrying characterization of the synthesized samples. I am also thankful to all the technical, non-teaching as well as office staffs of the School of Material Sciences and Technology, IIT (BHU) Varanasi for their assistance and support whenever required.

*My appreciation also goes to my labmates for their great help during my PhD journey- Dr. Bishnu Pada Majee, Dr. Shanu Mishra, Mr. Prince Kumar Maurya, Mr. Jay Deep Gupta, Mr. Rohit Kumar Gupta, Ms. Priyanka Jangra, Ms. Antima Pandey, Mr. Ankit Raj and my M. Tech juniors- Nilesh, Vishal, Shweta, Somesh, Yogesh, Himanshu, Shiksha, Vikash, Kundan, Pankaj, Sakshi, Sanghamitra and Swatendra. I am extremely thankful to my friends for making my stay here enjoyable and for their time-to-time encouragement during my Ph. D. journey - Ms. Asha Arya, Mrs. Priya Singh, Mr. Pawan Ojha, Ms. Priyanka Soni, Mrs. Neelam Sharma, Mr. Shashank Shekhar Shukla and other whoever helped me in this period. I could not be supposed to have a better friendly environment for my PhD life at IIT (BHU).*

*Finally, my deepest gratitude to my family, without whom this thesis could not be possible. I am thankful to my husband Mr. Abhishek Singh for his support and motivation at every step of my life. I am lucky to thank my elder brother Mr. Amit Kumar Singh, sister-in-law Mrs. Shweta Singh, elder sister Amita Singh and brother-in-law Mr. Ganesh Dutt Singh for providing me love, support, happiness and direction in life whenever I needed. My heartfelt gratitude is extended to the soul of my life- “my parents”- Mrs. Shashi Singh and Mr. Chandra Prakash Singh, for their constant encouragements, moral support and blessing at every step of my life that cannot be expressed in words. I genuinely feel that this thesis belongs to them more than to me. I would also like to express my heart-felt gratitude towards my parents in law- Mrs. Sumitra Singh and Mr. Virendra Pratap Singh for their love, support and blessings.*

*In the end, my sincere gratitude to the MHRD for providing me the fellowship, training, a wonderful learning experience and a chance to collaborate with the people with great expertise in the field outside my university.*

(Ankita Singh)

*Dedicated to my beloved parents*

## List of Figures

---

<b>Figure 1.1</b> Periodic table showing transition metal and chalcogen elements [7].....	2
<b>Figure 1.2</b> Schematic diagram showing the different polytypes of MoS <sub>2</sub> [8].....	3
<b>Figure 1.3</b> Schematic diagram showing the applications of MoS <sub>2</sub> nanostructures in various fields.....	18
<b>Figure 2.1</b> Schematic showing the different synthesis methods of MoS <sub>2</sub> .....	26
<b>Figure 2.2</b> Schematic illustration of CVD setup for the synthesis of MoS <sub>2</sub> film.....	27
<b>Figure 2.3</b> Schematic outlining the different optimized MoS <sub>2</sub> films along with their growth conditions.....	30
<b>Figure 2.4</b> Schematic diagram of optical microscope [83].....	31
<b>Figure 2.5</b> Optical image of CVD synthesized (a) different layered (1L, 3L and 5L) triangular MoS <sub>2</sub> /SiO <sub>2</sub> -Si, (b) H-MoS <sub>2</sub> /SiO <sub>2</sub> -Si and (c) H-MoS <sub>2</sub> /FTO.....	32
<b>Figure 2.6</b> Schematic diagram of scanning electron microscope (SEM) [87].....	33
<b>Figure 2.7</b> Schematic showing the interaction of electron beam with sample in SEM [87]...33	
<b>Figure 2.8</b> SEM images of (a) different layered triangular MoS <sub>2</sub> /SiO <sub>2</sub> -Si, (b) H-MoS <sub>2</sub> /SiO <sub>2</sub> -Si, (c) V-MoS <sub>2</sub> /SiO <sub>2</sub> -Si, (d) H-MoS <sub>2</sub> /FTO and (e) V-MoS <sub>2</sub> /Si.....	34
<b>Figure 2.9</b> Schematic diagram of atomic force microscope (AFM) [90].....	35
<b>Figure 2.10</b> The AFM image and corresponding height profile of (a) 1L, (b) 3L and (c) 5L triangular MoS <sub>2</sub> /SiO <sub>2</sub> -Si, (d) H-MoS <sub>2</sub> /SiO <sub>2</sub> -Si and (e) H-MoS <sub>2</sub> /FTO.....	36
<b>Figure 2.11</b> Schematic representation of the various scattering process: Rayleigh, stokes and anti-stokes Raman scattering [95].....	37
<b>Figure 2.12</b> Schematic diagram of Raman spectrometer.....	38
<b>Figure 2.13</b> Raman spectra of (a, c) 1L, 3L and 5L triangular MoS <sub>2</sub> /SiO <sub>2</sub> -Si and (b, d) H-MoS <sub>2</sub> /FTO, V-MoS <sub>2</sub> /Si, V-MoS <sub>2</sub> /SiO <sub>2</sub> -Si and H-MoS <sub>2</sub> /SiO <sub>2</sub> -Si, using 532 and 633 nm excitation wavelength.....	39
<b>Figure 2.14</b> Schematic representation of the photoluminescence (PL) spectroscopy [98].....	40
<b>Figure 2.15</b> (a) PL spectra of (a) 1L, 3L and 5L triangular MoS <sub>2</sub> /SiO <sub>2</sub> -Si and (b) H-MoS <sub>2</sub> /FTO, V-MoS <sub>2</sub> /Si, V-MoS <sub>2</sub> /SiO <sub>2</sub> -Si and H-MoS <sub>2</sub> /SiO <sub>2</sub> -Si, using 532 nm excitation wavelength.....	41
<b>Figure 2.16</b> (a) Schematic diagram of UV-Visible spectrophotometer [100].....	42
<b>Figure 2.17</b> UV-vis absorption spectra of H-MoS <sub>2</sub> /FTO, V-MoS <sub>2</sub> /Si, V-MoS <sub>2</sub> /SiO <sub>2</sub> -Si and H-MoS <sub>2</sub> /SiO <sub>2</sub> -Si.....	43

<b>Figure 3.1</b> (a) Top and side view of 1H-MoS <sub>2</sub> . (b) Unit cell of bulk MoS <sub>2</sub> . (c) Atomic displacement vector of Raman active modes. (d) The 2D first BZ with high-symmetry points.....	47
<b>Figure 3.2</b> (a)-(f) Electronic band structure and corresponding total DOS for 1 to 6L MoS <sub>2</sub> , respectively. The blue arrow shows the direct transition while the green arrow shows the indirect excitonic transition. The solid arrow shows the dominant transition among the direct and indirect ones.....	49
<b>Figure 3.3</b> Variation of bandgap (direct and indirect) as a function of layer number.....	50
<b>Figure 3.4</b> (a) Layer dependent Raman spectra (Lorentzian fitted). (b) Layer dependent frequencies of E <sub>12g</sub> and A <sub>1g</sub> Raman active modes and their differences. (c) PL spectra of different layers of MoS <sub>2</sub> (Gaussian fitted). (d) Schematic showing the A and B excitons in MoS <sub>2</sub> . (e) Variation of intensity and bandgap of A-exciton as a function of layer number.....	52
<b>Figure 3.5</b> Schematic showing the setup for temperature-dependent PL study.....	53
<b>Figure 3.6</b> (a) Temperature-dependent PL spectra of 1L, 3L and 5L triangular MoS <sub>2</sub> /SiO <sub>2</sub> -Si from 93-300 K (Gaussian fitted).....	54
<b>Figure 3.7</b> Variation of normalized integrated PL intensity and bandgap for A exciton of (a, b) 1L, (c, d) 3L and (e, f) 5L MoS <sub>2</sub> /SiO <sub>2</sub> -Si with temperature.....	56
<b>Figure 3.8</b> The variation of (a) spin orbit coupling energy (E <sub>SO</sub> ) and (b) FWHM for 1L, 3L and 5L triangular MoS <sub>2</sub> /SiO <sub>2</sub> -Si with temperature. The error bar presents the standard deviation.....	58
<b>Figure 3.9</b> Temperature-dependent PL spectra of H-MoS <sub>2</sub> /SiO <sub>2</sub> -Si (Gaussian fitted) from (a) 80 K to 230 K and (b) 260 K to 323 K. (c) Variation of normalized integrated PL intensity and the solid line shows the fitting using Arrhenius equation. (d) Variation of bandgap with temperature. The solid line shows the fitting to Varshni equation and the dotted line shows the fitting to O' Donnell and Chen equation. Variation of (e) E <sub>SO</sub> and (f) FWHM for H-MoS <sub>2</sub> /SiO <sub>2</sub> -Si with temperature. The error bar presents the standard deviation.....	59
<b>Figure 3.10</b> Temperature-dependent PL spectra of V-MoS <sub>2</sub> /SiO <sub>2</sub> -Si (Gaussian fitted) from (a) 80 K to 230 K and (b) 260 K to 323 K. (c) Variation of normalized integrated PL intensity and the solid line shows the fitting using Arrhenius equation. (d) Variation of bandgap with temperature. The solid line shows the fitting to Varshni equation and the dotted line shows the fitting to O' Donnell and Chen equation. Variation of (e) E <sub>SO</sub> and (f) FWHM for V-MoS <sub>2</sub> /SiO <sub>2</sub> -Si with temperature. The error bar presents the standard deviation.....	61
<b>Figure 3.11</b> Temperature-dependent PL spectra of H-MoS <sub>2</sub> /FTO (Gaussian fitted) from (a) 80 K to 230 K and (b) 260 K to 323 K. (c) Variation of normalized integrated PL intensity and the solid line shows the fitting using Arrhenius equation. (d) Variation of bandgap with temperature. The solid line shows the fitting to Varshni equation and the dotted line shows the fitting to O' Donnell and Chen equation. Variation of (e) E <sub>SO</sub> and (f) FWHM for H-MoS <sub>2</sub> /FTO with temperature. The error bar presents the standard deviation.....	63

**Figure 4.1** Symmetry operations in 1L (odd L) and 2L (even L) 2H-MoS<sub>2</sub>. (a, d) shows the top view for L=1 and 2 respectively. (b, e) shows the side view of respective layers with C<sub>3</sub> symmetry operation along the marked axis and red color circle represents the σ<sub>h</sub> reflection plane. The black dot at the centre in (e) illustrates the inversion symmetry. (c, f) shows three C<sub>2</sub>' symmetry along the red dotted line in the xy plane, σ<sub>v</sub> and σ<sub>d</sub> operation is shown by the mirror plane.....67

**Figure 4.2** Schematic showing the phonon vibrations in (a) 1L and (b) 2L MoS<sub>2</sub>. (c) Each phonon mode in 1L MoS<sub>2</sub> are split into two phonon modes in 2L MoS<sub>2</sub>.....69

**Figure 4.3** (a-f) Phonon dispersion curve along with phonon DOS for 1 to 6L MoS<sub>2</sub>.....71

**Figure 4.4** Schematic diagram depicting the experimental setup with backscattering geometry for demonstrating the ARPRS study of CVD grown triangular MoS<sub>2</sub>.....73

**Figure 4.5** (a) Optical image of CVD grown triangular MoS<sub>2</sub>/SiO<sub>2</sub>-Si. (b-d) Confocal Raman mapping of 1L, 3L and 5L triangular MoS<sub>2</sub>. The corresponding optical image is shown in the inset.....74

**Figure 4.6** Polarized Raman spectra of 1L CVD grown triangular MoS<sub>2</sub> nanostructure from (a) θ = 0° to 90°, (b) 100° to 180°, (c) 190° to 270° and (d) 280° to 360°, at an interval of 10°, obtained using 532 nm excitation.....79

**Figure 4.7** Polarized Raman spectra of 3L CVD grown triangular MoS<sub>2</sub> nanostructure from (a) θ = 0° to 90°, (b) 100° to 180°, (c) 190° to 270° and (d) 280° to 360°, at an interval of 10°, obtained using 532 nm excitation.....79

**Figure 4.8** Polarized Raman spectra of 5L CVD grown triangular MoS<sub>2</sub> nanostructure from (a) θ = 0° to 90°, (b) 100° to 180°, (c) 190° to 270° and (d) 280° to 360°, at an interval of 10°, obtained using 532 nm excitation.....80

**Figure 4.9** Polar plots of layer dependent (1L, 3L and 5L) triangular MoS<sub>2</sub> for (c) E<sup>1</sup><sub>2g</sub> and (d) A<sub>1g</sub> phonon mode.....80

**Figure 4.10** Polarized Raman spectra of 3L CVD grown triangular MoS<sub>2</sub> nanostructure from (a) θ = 0° to 90°, (b) 100° to 180°, (c) 190° to 270° and (d) 280° to 360°, at an interval of 10°, obtained using 633 nm excitation.....81

**Figure 4.11** Polarized Raman spectra of 3L CVD grown triangular MoS<sub>2</sub> nanostructure from (a) θ = 0° to 90°, (b) 100° to 180°, (c) 190° to 270° and (d) 280° to 360°, at an interval of 10°, obtained using 633 nm excitation.....82

**Figure 4.12** Polar plots of layer dependent (3L and 5L) MoS<sub>2</sub> for (a) E<sup>1</sup><sub>2g</sub>, (b) A<sub>1g</sub>, (c) A<sub>1g</sub>(M) – LA (M) and (d) 2LA(M) phonon modes.....82

**Figure 4.13** Polarized Raman spectra of H-MoS<sub>2</sub>/SiO<sub>2</sub>-Si from (a) θ = 0° to 90°, (b) 100° to 180°, (c) 190° to 270° and (d) 280° to 360°, at an interval of 10°, obtained using 532 nm excitation. (e) Polar plots of H-MoS<sub>2</sub>/SiO<sub>2</sub>-Si for E<sup>1</sup><sub>2g</sub> and A<sub>1g</sub> phonon mode.....84

**Figure 4.14** Polarized Raman spectra of H-MoS<sub>2</sub>/SiO<sub>2</sub>-Si from (a) θ = 0° to 90°, (b) 100° to 180°, (c) 190° to 270° and (d) 280° to 360°, at an interval of 10°, obtained using 633 nm

excitation. (e) Polar plots of H-MoS<sub>2</sub>/SiO<sub>2</sub>-Si for E<sup>1</sup><sub>2g</sub>, A<sub>1g</sub>, A<sub>1g</sub>(M) – LA (M) and 2LA(M) phonon mode.....86

**Figure 4.15** (a) SEM image of V-MoS<sub>2</sub>/SiO<sub>2</sub>-Si. Polarized Raman spectra of V-MoS<sub>2</sub>/SiO<sub>2</sub>-Si from (b) 0° to 90°, (c) 100° to 180°, (d) 190° to 270° and (e) 280° to 360°, at an interval of 10°, obtained using 532 nm excitation (f) Polar plots of V-MoS<sub>2</sub>/SiO<sub>2</sub>-Si for E<sup>1</sup><sub>2g</sub> and A<sub>1g</sub> phonon mode with 532 nm excitation.....88

**Figure 4.16** Polarized Raman spectra of V-MoS<sub>2</sub>/SiO<sub>2</sub>-Si from (a) 0° to 90°, (b) 100° to 180°, (c) 190° to 270° and (d) 280° to 360°, at an interval of 10°, obtained using 633 nm excitation. (e) Polar plots of V-MoS<sub>2</sub>/SiO<sub>2</sub>-Si for E<sup>1</sup><sub>2g</sub>, A<sub>1g</sub>, A<sub>1g</sub>(M) – LA (M) and 2LA(M) phonon mode.....89

**Figure 4.17** Polarized Raman spectra of H-MoS<sub>2</sub>/FTO from (a)  $\theta = 0^\circ$  to 90°, (b) 100° to 180°, (c) 190° to 270° and (d) 280° to 360°, at an interval of 10°, obtained using 532 nm excitation. (e) Polar plots of H-MoS<sub>2</sub>/FTO for E<sup>1</sup><sub>2g</sub> and A<sub>1g</sub> phonon mode.....91

**Figure 4.18** Polarized Raman spectra of H-MoS<sub>2</sub>/FTO from (a)  $\theta = 0^\circ$  to 90°, (b) 100° to 180°, (c) 190° to 270° and (d) 280° to 360°, at an interval of 10°, obtained using 633 nm excitation. (e) Polar plots of H-MoS<sub>2</sub>/FTO for E<sup>1</sup><sub>2g</sub>, A<sub>1g</sub>, A<sub>1g</sub>(M) – LA (M) and 2LA(M) phonon mode.....92

**Figure 5.1** Schematic showing the setup for optothermal Raman study.....97

**Figure 5.2** Temperature-dependent phonon response from 80 to 193 K and from 213 to 333 K of (a, b) 1L, (c, d) 3L and (e, f) 5L CVD grown triangular MoS<sub>2</sub>/SiO<sub>2</sub>-Si using 50x LWD lens.....99

**Figure 5.3** Variations of (a) peak position and (b) FWHM of E<sup>1</sup><sub>2g</sub> and A<sub>1g</sub> modes with temperature for 1L, 3L and 5L triangular MoS<sub>2</sub>/SiO<sub>2</sub>-Si.....100

**Figure 5.4** The modelling of temperature-dependent Raman shift (red solid line) and individual theoretical contributions to experimental results (black square) from pure thermal expansion (green solid line), three-phonon (blue solid line) and four-phonon (pink solid line) of E<sup>1</sup><sub>2g</sub> and A<sub>1g</sub> modes of (a, b) 1L, (c, d) 3L and (e, f) 5L triangular MoS<sub>2</sub>/SiO<sub>2</sub>-Si.....103

**Figure 5.5** Power-dependent Raman spectra of (a) 1L, (b) 3L and (c) 5L triangular MoS<sub>2</sub>/SiO<sub>2</sub>-Si using 50x LWD objective lens. (d) Variations of peak positions with incident laser power of E<sup>1</sup><sub>2g</sub> and A<sub>1g</sub> modes for 1L, 3L and 5L MoS<sub>2</sub>/SiO<sub>2</sub>-Si .....105

**Figure 5.6** Variations of FWHM of E<sup>1</sup><sub>2g</sub> and A<sub>1g</sub> phonon modes with incident laser power for CVD grown triangular (a) 1L, (b) 3L and (c) 5L MoS<sub>2</sub>/SiO<sub>2</sub>-Si using 50x LWD lens.....105

**Figure 5.7** Power-dependent Raman spectra of (a) 1L, (b) 3L and (c) 5L triangular MoS<sub>2</sub>/SiO<sub>2</sub>-Si using 100x objective lens. (d) Variations of peak positions with incident laser power of E<sup>1</sup><sub>2g</sub> and A<sub>1g</sub> modes for 1L, 3L and 5L MoS<sub>2</sub>/SiO<sub>2</sub>-Si .....106

**Figure 5.8** Variations of FWHM for E<sup>1</sup><sub>2g</sub> and A<sub>1g</sub> phonon modes with incident laser power for CVD grown triangular (a) 1L, (b) 3L and (c) 5L MoS<sub>2</sub>/SiO<sub>2</sub>-Si using 100x objective lens...107

**Figure 5.9** Temperature-dependent Raman spectra from (a) 80 to 193 K and (b) 213 to 333 K of H-MoS<sub>2</sub>/SiO<sub>2</sub>-Si. Variation in (c) Raman peak positions and (d) FWHM with temperature of H-MoS<sub>2</sub>/SiO<sub>2</sub>-Si. Individual contributions to three-phonon, four-phonon and thermal expansion in (e) E<sup>1</sup><sub>2g</sub> and (f) A<sub>1g</sub> phonon modes of H-MoS<sub>2</sub>/SiO<sub>2</sub>-Si .....113

**Figure 5.10** (a, b) Power dependent Raman spectra, (c, d) variation of peak position with laser power and (e, f) variation of FWHM with laser power for both the phonon modes with 50x LWD and 100x objective lens, respectively on H-MoS<sub>2</sub>/SiO<sub>2</sub>-Si.....115

**Figure 5.11** Temperature-dependent Raman spectra from (a) 80 to 193 K and (b) 213 to 333 K of V-MoS<sub>2</sub>/SiO<sub>2</sub>-Si. Variation in (c) Raman peak positions and (d) FWHM with temperature of V-MoS<sub>2</sub>/SiO<sub>2</sub>-Si. Individual contributions to three-phonon, four-phonon and thermal expansion in (e) E<sup>1</sup><sub>2g</sub> and (f) A<sub>1g</sub> phonon modes of V-MoS<sub>2</sub>/SiO<sub>2</sub>-Si.....118

**Figure 5.12** (a, b) Power-dependent Raman spectra, (c, d) variation of peak position with laser power and (e, f) variation of FWHM with laser power for both the phonon modes with 50x LWD and 100x objective lens, respectively on V-MoS<sub>2</sub>/SiO<sub>2</sub>-Si.....120

**Figure 5.13** Temperature-dependent Raman spectra from (a) 80 to 193 K and (b) 213 to 333 K of H-MoS<sub>2</sub>/FTO. Variation in (c) Raman peak positions and (d) FWHM with temperature of H-MoS<sub>2</sub>/FTO. Individual contributions to three-phonon, four-phonon and thermal expansion in (e) E<sup>1</sup><sub>2g</sub> and (f) A<sub>1g</sub> phonon modes of H-MoS<sub>2</sub>/FTO.....123

**Figure 5.14** (a, b) Power-dependent Raman spectra, (c, d) variation of peak position with laser power and (e, f) variation of FWHM with laser power for both the phonon modes with 50x LWD and 100x objective lens, respectively.....125

**Figure 6.1** Schematic illustrating the (a) SERS process, (b) Electromagnetic enhancement and (c) Chemical enhancement.....129

**Figure 6.2** Photographs showing the different concentrations of (a) bilirubin biomolecule from 10<sup>-3</sup> to 10<sup>-12</sup> M and (b) vitamin B<sub>12</sub> (cyanocobalamin) from 10<sup>-3</sup> to 10<sup>-9</sup> M.....131

**Figure 6.3** Raman spectra of (a) bulk bilirubin collected using 633 nm excitation laser and (b) bulk vitamin B<sub>12</sub> biomolecules collected using 532 nm excitation laser.....132

**Figure 6.4** SEM images of (a,b) H-MoS<sub>2</sub>/FTO, (c,d) V-MoS<sub>2</sub>/Si, (e,f) V-MoS<sub>2</sub>/SiO<sub>2</sub>-Si and (g,h) H-MoS<sub>2</sub>/SiO<sub>2</sub>-Si.....135

**Figure 6.5** SERS spectra of bilirubin biomolecule at different concentrations on (a,b) H-MoS<sub>2</sub>/FTO, (c,d) V-MoS<sub>2</sub>/Si, (e,f) V-MoS<sub>2</sub>/SiO<sub>2</sub>-Si and (g) H-MoS<sub>2</sub>/SiO<sub>2</sub>-Si SERS substrates. (h) Raman intensity of characteristic peak versus bilirubin concentrations on these substrates.....137

**Figure 6.6** (a) SERS spectrum and mapping of (b) MoS<sub>2</sub> (~457 cm<sup>-1</sup>, shown by red color) and (c) bilirubin (~1613 cm<sup>-1</sup>, shown by green color) on H-MoS<sub>2</sub>/FTO. Inset of (a) shows the SERS mapping of bilirubin adsorbed over H-MoS<sub>2</sub>/FTO.....138

<b>Figure 6.7</b> (a) SERS spectrum and mapping of (b) MoS <sub>2</sub> (~457 cm <sup>-1</sup> , shown by red color) and (c) bilirubin (~1612 cm <sup>-1</sup> , shown by green color) on V-MoS <sub>2</sub> /Si. Inset of (a) shows the SERS mapping of bilirubin adsorbed over V-MoS <sub>2</sub> /Si.....	139
<b>Figure 6.8</b> (a) SERS spectrum and mapping of (b) MoS <sub>2</sub> (~457 cm <sup>-1</sup> , shown by red color) and (c) bilirubin (~1611 cm <sup>-1</sup> , shown by green color) on V-MoS <sub>2</sub> /SiO <sub>2</sub> -Si. Inset of (a) shows the SERS mapping of bilirubin adsorbed over V-MoS <sub>2</sub> /SiO <sub>2</sub> -Si.....	140
<b>Figure 6.9</b> (a) SERS spectrum and mapping of (b) MoS <sub>2</sub> (~457 cm <sup>-1</sup> , shown by red color) and (c) bilirubin (~1613 cm <sup>-1</sup> , shown by green color) on H-MoS <sub>2</sub> /SiO <sub>2</sub> -Si. Inset of (a) shows the SERS mapping of bilirubin adsorbed over H-MoS <sub>2</sub> /SiO <sub>2</sub> -Si.....	141
<b>Figure 6.10</b> SERS spectra of vitamin B <sub>12</sub> at different concentrations on (a) H-MoS <sub>2</sub> /FTO (10 <sup>-3</sup> to 10 <sup>-8</sup> M), (b) V-MoS <sub>2</sub> /Si (10 <sup>-3</sup> to 10 <sup>-8</sup> M), (c) V-MoS <sub>2</sub> /SiO <sub>2</sub> -Si (10 <sup>-3</sup> to 10 <sup>-7</sup> M) and (d) H-MoS <sub>2</sub> /SiO <sub>2</sub> -Si (10 <sup>-3</sup> to 10 <sup>-6</sup> M). (e) Raman intensity of characteristic peak versus vitamin B <sub>12</sub> concentrations on these substrates.....	142
<b>Figure 6.11</b> (a) SERS spectrum and mapping of (b) MoS <sub>2</sub> (~406 cm <sup>-1</sup> , shown by red color) and (c) vitamin B <sub>12</sub> (~1499 cm <sup>-1</sup> , shown by green color) on H-MoS <sub>2</sub> /FTO. Inset of (a) shows the SERS mapping of vitamin B <sub>12</sub> adsorbed over H-MoS <sub>2</sub> /FTO.....	143
<b>Figure 6.12</b> (a) SERS spectrum and mapping of (b) MoS <sub>2</sub> (~406 cm <sup>-1</sup> , shown by red color) and (c) vitamin B <sub>12</sub> (~1497 cm <sup>-1</sup> , shown by green color) on V-MoS <sub>2</sub> /Si. Inset of (a) shows the SERS mapping of vitamin B <sub>12</sub> adsorbed over V-MoS <sub>2</sub> /Si.....	144
<b>Figure 6.13</b> (a) SERS spectrum and mapping of (b) MoS <sub>2</sub> (~406 cm <sup>-1</sup> , shown by red color) and (c) vitamin B <sub>12</sub> (~1498 cm <sup>-1</sup> , shown by green color) on V-MoS <sub>2</sub> /SiO <sub>2</sub> -Si. Inset of (a) shows the SERS mapping of vitamin B <sub>12</sub> adsorbed over V-MoS <sub>2</sub> /SiO <sub>2</sub> -Si.....	145
<b>Figure 6.14</b> (a) SERS spectrum and mapping of (b) MoS <sub>2</sub> (~406 cm <sup>-1</sup> , shown by red color) and (c) vitamin B <sub>12</sub> (~1501 cm <sup>-1</sup> , shown by green color) on H-MoS <sub>2</sub> /SiO <sub>2</sub> -Si. Inset of (a) shows the SERS mapping of vitamin B <sub>12</sub> adsorbed over H-MoS <sub>2</sub> /SiO <sub>2</sub> -Si.....	146
<b>Figure 6.15</b> Schematic of the coupling scheme for the B-term: CT resonance is coupled with molecular resonance or exciton resonance via h <sub>CK</sub> or h <sub>IV</sub> , and, C-term: CT resonance is coupled with molecular resonance or exciton resonance via h <sub>IV</sub> or h <sub>CK</sub> .....	148
<b>Figure 6.16</b> Schematic energy band diagram for charge transfer among FTO, H-MoS <sub>2</sub> and biomolecule.....	149
<b>Figure 6.17</b> The PL spectra of (a) H-MoS <sub>2</sub> /FTO, (b) V-MoS <sub>2</sub> /Si, (c) V-MoS <sub>2</sub> /SiO <sub>2</sub> -Si and (d) H-MoS <sub>2</sub> /SiO <sub>2</sub> -Si SERS substrates with and without vitamin B <sub>12</sub> .....	151
<b>Figure 6.18</b> Raman spectra of 10 <sup>-3</sup> M concentration of (a) bilirubin and (b) vitamin B <sub>12</sub> over FTO coated glass, Si and SiO <sub>2</sub> -Si substrate.....	152
<b>Figure 6.19</b> Temperature-dependent SERS from 323 to 260 K and from 230 to 80 K of (a, b) 10 <sup>-9</sup> M bilirubin on H-MoS <sub>2</sub> /FTO, (c, d) 10 <sup>-9</sup> M bilirubin on V-MoS <sub>2</sub> /Si, (e, f) 10 <sup>-7</sup> M bilirubin on V-MoS <sub>2</sub> /SiO <sub>2</sub> -Si and (g, h) 10 <sup>-6</sup> M bilirubin on H-MoS <sub>2</sub> /SiO <sub>2</sub> -Si.....	158

**Figure 6.20** Temperature-dependent SERS from 323 to 260 K and from 230 to 80 K of (a, b)  $10^{-6}$  M vitamin B<sub>12</sub> on H-MoS<sub>2</sub>/FTO, (c, d)  $10^{-6}$  M vitamin B<sub>12</sub> on V-MoS<sub>2</sub>/Si, (e, f)  $10^{-5}$  M vitamin B<sub>12</sub> on V-MoS<sub>2</sub>/ SiO<sub>2</sub>-Si and (g, h)  $10^{-4}$  M vitamin B<sub>12</sub> on H-MoS<sub>2</sub>/SiO<sub>2</sub>-Si.....159

**Figure 6.21** Raman intensity versus temperature of (a) bilirubin and (b) vitamin B<sub>12</sub> on H-MoS<sub>2</sub>/FTO, V-MoS<sub>2</sub>/Si, V-MoS<sub>2</sub>/SiO<sub>2</sub>-Si and H-MoS<sub>2</sub>/SiO<sub>2</sub>-Si.....160

## List of Tables

---

<b>Table 3.1</b> Calculated fitting parameters defining the A exciton for 1L, 3L and 5L MoS <sub>2</sub> , obtained by fitting the bandgap using O'Donnell and Chen equation at different temperatures.....	57
<b>Table 4.1</b> Character table for D <sub>3h</sub> point group.....	68
<b>Table 4.2</b> Character table for D <sub>3d</sub> point group.....	68
<b>Table 4.3</b> Comparison of theoretically obtained frequencies of optical phonon modes at $\Gamma$ point in 1L MoS <sub>2</sub> with experimentally reported data (in units of cm <sup>-1</sup> ).....	72
<b>Table 5.1</b> The fitting parameters A and B for E <sup>1</sup> <sub>2g</sub> and A <sub>1g</sub> phonon mode in three- and four-phonon scattering process.....	103
<b>Table 5.2</b> First order power- and temperature-dependent coefficients for both the E <sup>1</sup> <sub>2g</sub> and A <sub>1g</sub> phonon modes of supported 1L, 3L and 5L MoS <sub>2</sub> .....	107
<b>Table 5.3</b> Absorption coefficient, thermal resistance, interfacial thermal conductance and thermal conductivities of 1L, 3L and 5L MoS <sub>2</sub> .....	109
<b>Table 5.4</b> Thermal conductivity of different MoS <sub>2</sub> films using the optothermal Raman technique.....	110
<b>Table 6.1</b> Assignments of bands of bilirubin biomolecules using 633 nm excitation [198, 220].....	132
<b>Table 6.2</b> Assignments of bands of vitamin B <sub>12</sub> biomolecules using 532 nm excitation [221, 222].....	133
<b>Table 6.3</b> I <sub>Raman</sub> and I <sub>SERS</sub> for both the biomolecules on different substrates.....	152
<b>Table 6.4</b> The values of R obtained on different SERS substrates.....	153
<b>Table 6.5</b> Calculated number of molecules per $\mu\text{m}^2$ (at lowest concentration) for bilirubin and vitamin B <sub>12</sub> over different substrates at lowest concentration.....	154
<b>Table 6.6</b> EF for different biomolecules on different SERS substrates.....	155
<b>Table 6.7</b> Comparison of the SERS detection limit of bilirubin and vitamin B <sub>12</sub> over different substrates with different analytical methods.....	155

## List of Abbreviation

---

AFM	Atomic force microscopy
ARPRS	Angle resolved polarized Raman spectroscopy
BSE	Backscattered electrons
BZ	Brillouin zone
CB	Conduction band
CM	Chemical enhancement
CT	Charge transfer
CVD	Chemical vapor deposition
DFT	Density functional theory
DFPT	Density functional perturbation theory.
DOS	Density of states
DP	Deformation potential
EF	Enhancement factor
EM	Electromagnetic enhancement
eV	Electron volt
FI	Fröhlich interaction
FTO	Fluorine-doped tin oxide
FWHM	Full width at half-maximum
HOMO	Highest occupied molecular orbitals
ILC	Interlayer coupling
LSPR	Localized surface plasmon resonance
LUMO	Lowest unoccupied molecular orbitals
LWD	Long working distance
MBE	Molecular beam epitaxy
MOCVD	Metal-organic chemical vapor deposition

MoS <sub>2</sub>	Molybdenum disulfide
MFC	Mass flow controller
MW	Mega watt
N.A.	Numerical aperture
OTR	Optothermal Raman
PL	Photoluminescence
PECVD	Plasma-assisted chemical vapor deposition
PICT	Photo-induced charge transfer
PVD	Physical vapor deposition
RT	Room temperature
Si	Silicon
SiO <sub>2</sub>	Silicon dioxide
sccm	Standard cubic centimeter per minute
SERS	Surface enhanced Raman spectroscopy
SE	Secondary electrons
SEM	Scanning electron microscopy
SOC	Spin orbit coupling
2D	Two dimensional
TDTR	Time-domain thermos-reflectance
TMDs	Transition metal dichalcogenides
VB	Valence band

## List of Symbols

---

$\alpha$	Absorption coefficient
$N_A$	Avogadro constant
$(\Delta\omega)_{\text{anh}}$	Anharmonic phonon-phonon interaction
$k_B$	Boltzmann's constant.
$\langle\hbar\omega\rangle$	Average phonon energy involved in the electron-phonon interaction
$\omega_0$	Extrapolated peak position of phonon modes at 0 K
$n$	Degeneracy
$E_g(0)$	Energy of A exciton at 0 K
$E_g(T)$	Energy of A exciton at temperature T
$\chi_P$	First-order power-dependent coefficient
$\chi_T$	First order temperature coefficient
$\gamma$	Grüneisen parameter
$g$	Interfacial thermal conductance
$\alpha_a$	In-plane thermal expansion coefficient
$\alpha_c$	Out of-plane thermal expansion coefficient
$\hat{\mathbf{g}}_i$	Polarization of the incident laser light
$\hat{\mathbf{g}}_s$	Polarization of the scattered laser light
$I_0$	PL intensity at 0 K
$S$	Strength of the electron-phonon coupling
$E_{\text{SO}}$	Spin orbit coupling energy
$I_{\text{PL}}(T)$	Temperature-dependent PL intensity
$k_{\text{rad}}(T)$	Temperature-dependent radiative recombination rates
$k_{\text{nonrad}}(T)$	Temperature-dependent nonradiative recombination rates
$k_s$	Thermal conductivity
$\alpha_T$	Thermal expansion coefficient
$(\Delta\omega)_{\text{latt}}$	Thermal expansion of the lattice
$R_m$	Thermal resistance
$\beta$	Varshni coefficients related to the electron-phonon interaction.
$\lambda$	Wavelength